# Inversion of the Dioxolanyl Radical: An Experimental and Theoretical Study[1]

**S. Deycard,[2] J. Lusztyk,* K. U. Ingold, F. Zerbetto,[3] M. Z. Zgierski, and W. Siebrand**

*Contribution from the Division of Chemistry, National Research Council of Canada, Ottawa, Ontario, Canada K1A 0R6.* *Received November 17, 1989*

**Abstract:** Dynamic EPR spectroscopy has been used to investigate the inversion of 1,3-dioxolan-2-yl and [2-D]-1,3-dioxolan-2-yl radicals. The former shows no detectable line broadening down to 93 K, which implies "instant" inversion on the EPR time scale, but the latter shows a temperature-dependent EPR spectrum from which the inversion rate constants have been deduced. These rate constants give rise to a curved Arrhenius plot which, together with the large primary isotope effect, indicates that the inversion proceeds by quantum-mechanical tunneling. To investigate the transition quantitatively, an ab initio UHF-MO calculation has been carried out, yielding the molecular geometry and the normal-mode frequencies in the equilibrium and transition state, as well as an inversion barrier height of ca. 2500 $cm^{-1}$. The inversion is found to be dominated by two vibrational degrees of freedom, namely, a ring-bending mode in addition to the $CH_\alpha$-bending mode. The potential of the latter mode is approximated by a modified quartic double-minimum potential. The former mode is treated semiclassically: it modifies the quartic potential via an anharmonic cross-term yielding a series of quartic potentials, one for each state of the ring-bending mode, weighted by the Boltzmann population of the state. The observed rate constants can be fitted accurately to the $CH_\alpha$-level splittings generated by this model. The resulting effective one-dimensional inversion barrier compares favorably with the corresponding barrier deduced quantum-chemically.

In a recent series of papers[4-7] we have employed chemical-trapping,[4] electron paramagnetic resonance (EPR) spectroscopy[5,6] and quantum-chemical calculations[6,7] to investigate the dynamics of the inversion of carbon-centered radicals in which the radical center is an integral part of a three-membered ring. For judiciously chosen radicals, the EPR method allows first-order rate constants for inversion, $k_{inv}$, to be measured over a range of temperatures, provided $10^5\ s^{-1} \lesssim k_{inv} \lesssim 10^8\ s^{-1}$. The exocyclic substituent attached to the radical center may be hydrogen, deuterium, a methyl group, etc. In principle, these measurements provide information on the inversion reaction pathway and its potential-energy barrier. To exploit fully the experimental data, we carry out quantum-chemical calculations on the radical's vibrational force field and use these results for dynamical calculations.

The cyclopropyl[4] and [1-D]cyclopropyl[8] radicals invert too rapidly at all temperatures for experimental study by the EPR method. However, the oxiran-2-yl and [2-D]oxiran-2-yl radicals invert at appropriate rates and provide a wealth of data for comparison with the quantum-chemical calculations.[6] For these radicals, inversion can be described as an essentially one-dimensional process that very clearly involves quantum-mechanical tunneling of the hydrogen or deuterium atom attached to the radical center. The second example of inversion, the 1-methylcyclopropyl radical,[5,7] turned out to be more complicated because strong coupling with methyl rotation makes inversion effectively a two-dimensional process. Hydrogen tunneling is involved in the methyl rotation, as would be expected. More interestingly, heavy atom (viz., methyl group) tunneling was also found to play a significant role in the inversion process.[7] However, near the high-temperature limit of the EPR method, methyl rotation becomes so rapid that the inversion could actually be treated as a quasi-one-dimensional problem.[7]

In the present paper, we extend these studies to the 1,3-dioxolan-2-yl (depicted in Figure 1) and the [2-D]-1,3-dioxolan-2-yl radicals. The former radical has been examined by EPR spectroscopy on several previous occasions.[9-12] The radical center is distinctly nonplanar and the hyperfine splitting (hfs) of the $\alpha$-hydrogen atom has been deduced to have a positive sign.[9,10] Furthermore, (low-level) quantum-chemical calculations have indicated that the five heavy atoms that together constitute the ring do not lie in one plane.[11] Vibrations of the five-membered ring are therefore expected to influence inversion at the radical center, such that inversion will be a multidimensional problem. Experimentally, we have extended Gaze and Gilbert's[11] observation that there is no detectable line broadening in 1,3-dioxolan-2-yl at temperatures as low as 146 K, to 93 K, which implies that inversion is too rapid to be directly measurable by the EPR method. However, it has been shown that substitution of a methyl group at the radical center, as in the 2-methyl-1,3-dioxolan-2-yl radical, reduces the rate of inversion to the point where the EPR spectrum at low temperatures ($T \lesssim 170$ K) shows hfs by two pairs of magnetically inequivalent $\gamma$-hydrogen atoms.[11,13,14] Temperature-dependent rate parameters, which follow the Arrhenius law, have been derived by comparison of measured and simulated EPR spectra.[13,14] The enthalpic barrier for inversion of the methyl group in this radical has been calculated as 5.6 ± 0.2 kcal/mol[13] and as 5.7 ± 0.2 kcal/mol.[14] These data, together with our own results on the three-membered-ring radicals,[4-7] suggest that the inversion rate for 1,3-dioxolan-2-yl will not be greatly outside the

**Table I.** Hyperfine Splittings (in Gauss) of 1,3-Dioxolan-2-yl and 1,3-Dioxolan-4-yl Radicals in Freon 13 at 179 ± 3 K

| radical | $a^{H(D)}$ $H_\alpha(D_\alpha)$ | $H_\beta$ | $H_\gamma(D_\gamma)$ | $a^{13C}$ $C_\alpha$ |
|---|---|---|---|---|
| 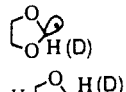 | 21.10 (3.22) | | 1.45, 4 H (1.45, 4 H) | 103[a] |
| 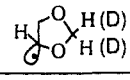 | 11.90 (11.90) | 27.3, 2 H (27.3, 2 H) | 1.65, 2 H (0.25, 2 D) | |

[a] At room temperature in water (ref 10).

(1) Issued as NRCC No. 31391.
(2) Canada-France Postdoctoral Exchange Fellow.
(3) NRCC Research Associate.
(4) Johnston, L. J.; Ingold, K. U. *J. Am. Chem. Soc.* **1986**, *108*, 2343-2348.
(5) Deycard, S.; Hughes, L.; Lusztyk, J.; Ingold, K. U. *J. Am. Chem. Soc.* **1987**, *109*, 4954-4960.
(6) Deycard, S.; Lusztyk, J.; Ingold, K. U.; Zerbetto, F.; Zgierski, M. Z.; Siebrand, W. *J. Am. Chem. Soc.* **1988**, *110*, 6721-6726.
(7) Zerbetto, F.; Zgierski, M. Z.; Siebrand, W. *J. Am. Chem. Soc.* **1989**, *111*, 2799-2802.
(8) See footnote 16 in ref 6.
(9) Dobbs, A. J.; Gilbert, B. C.; Norman, R. O. C. *J. Chem. Soc. A* **1971**, 124-135.
(10) Beckwith, A. L. J.; Tindall, P. K. *Aust. J. Chem.* **1971**, *24*, 2099-2116.
(11) Gaze, C.; Gilbert, B. C. *J. Chem. Soc., Perkin Trans. 2* **1977**, 1161-1168.
(12) Brunton, G.; Ingold, K. U.; Roberts, B. P.; Beckwith, A. L. J.; Krusic, P. J. *J. Am. Chem. Soc.* **1977**, *99*, 3177-3179.
(13) Kobayashi, S. O.; Simamura, O. *Chem. Lett.* **1973**, 699-702.
(14) Gaze, C.; Gilbert, B. C.; Symons, M. C. R. *J. Chem. Soc., Perkin Trans. 2* **1978**, 235-242.

0002-7863/90/1512-4284$02.50/0 Published 1990 by the American Chemical Society

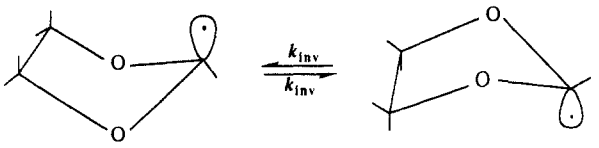


**Figure 1.** 1,3-Dioxolan-2-yl.

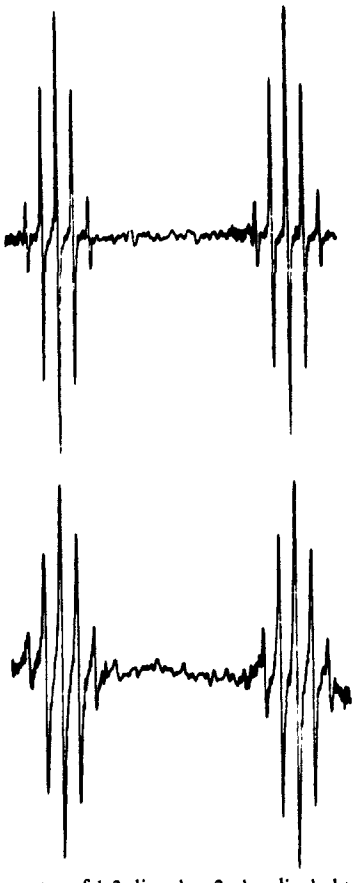

**Figure 2.** EPR spectra of 1,3-dioxolan-2-yl radical obtained during the photolysis of di-*tert*-butyl peroxide in the presence of 1,3-dioxolane in Freon 13 solvent at 181 (top) and 98 K (bottom).

range accessible to the EPR method. This, in turn, suggests that the rate of inversion of the $\alpha$-deuterium-substituted radical might be measurable by this technique, and this indeed turns out to be true.

We report herein temperature-dependent values of $k_{inv}$ for the [2-D]-1,3-dioxolan-2-yl radical and show that they do not fit the Arrhenius law. To interpret these experimental results, we have performed quantum-chemical calculations of the force field of the radical in several configurations relevant to the inversion process.

## Results

**EPR Experiments. 1,3-Dioxolan-2-yl.** This radical was generated directly in the cavity of a Varian E 104 EPR spectrometer by hydrogen atom abstraction from 1,3-dioxolane by photochemically generated *tert*-butoxyl radicals (from di-*tert*-butyl peroxide) in Freon 13 as solvent and at temperatures in the range 93–183 K. The EPR spectrum of this radical is shown in Figure 2 and the derived hfs, which are in good agreement with the literature,[9-12] are listed in Table I together with the hfs for the 1,3-dioxolan-4-yl radical, which is produced simultaneously but in considerably lower concentration than the radical of interest.[15] The spectrum of the 1,3-dioxolan-2-yl radical showed no temperature-dependent selective line broadening down to 93 K, indicating that inversion is rapid on the EPR time scale.

(15) The 4-yl radical is produced in higher concentrations relative to the 2-yl radical when photochemically generated $Me_3SiO^{\bullet}$ and $CF_3O^{\bullet}$ are used instead of $Me_3CO^{\bullet}$ radicals as the hydrogen (deuterium) atom abstracting agents. A study of the regioselectivity of alkoxyl radicals toward 1,3-dioxolane and other substrates will be reported elsewhere.

**Figure 3.** EPR spectra of [2-D]-1,3-dioxolan-2-yl and [2,2-$D_2$]-1,3-dioxolan-4-yl radicals obtained during the photolysis of di-*tert*-butyl peroxide in the presence of [2,2-$D_2$]-1,3-dioxolane in Freon 13 solvent at 174 (top) and 107 K (bottom).

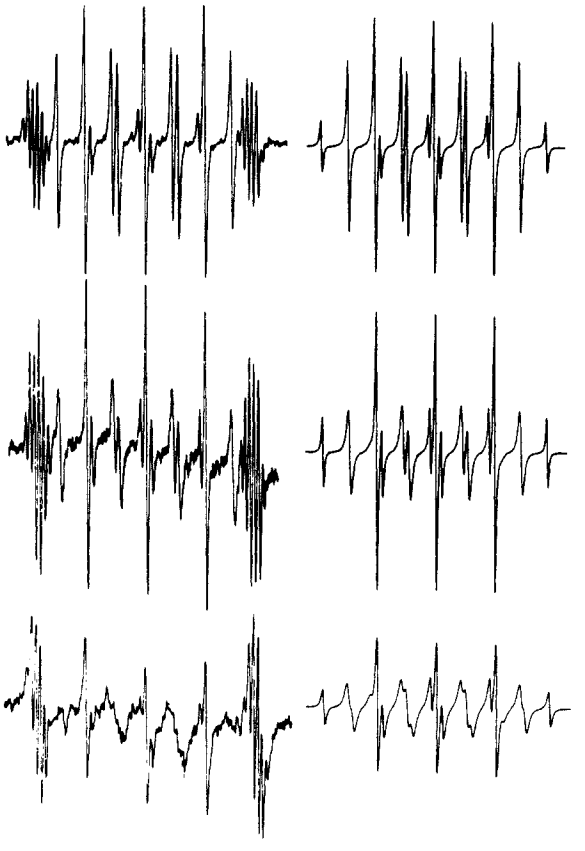

**Figure 4.** Comparison of observed (left) and simulated (right) EPR spectra of 1,3-dioxolan-2-yl radical obtained at 182 (top), 142 (middle), and 99 K (bottom). The highly resolved lines on the wings of the observed spectra belong to the [2,2-$D_2$]-1,3-dioxolan-4-yl radical.

**[2-D]-1,3-Dioxolan-2-yl.** This radical was produced as described above by deuterium atom abstraction, from [2,2-$D_2$]-1,3-dioxolane. Because of the deuterium isotope effect on abstraction, the yield of [2,2-$D_2$]-1,3-dioxolan-4-yl relative to [2-D]-1,3-dioxolan-2-yl was greater than was the case for abstraction from the nondeuterated substrate.[15] The spectra of the two deuterated radicals overlap slightly (see Figure 3) and the two outermost lines of the

**Table II.** Estimated Rate Constants for Inversion of [2-D]-1,3-Dioxolan-2-yl[a]

| $T$, K | $k^{D}_{inv}$, $s^{-1}$ | $T$, K | $k^{D}_{inv}$, $s^{-1}$ |
|---|---|---|---|
| 99 | $1.5 \times 10^6$ | 152 | $6.0 \times 10^6$ |
| 110 | $1.8 \times 10^6$ | 157 | $7.0 \times 10^6$ |
| 121 | $2.0 \times 10^6$ | 163 | $1.0 \times 10^7$ |
| 122 | $1.9 \times 10^6$ | 171 | $1.5 \times 10^7$ |
| 132 | $2.8 \times 10^6$ | 172 | $1.7 \times 10^7$ |
| 132 | $2.5 \times 10^6$ | 182 | $3.0 \times 10^7$ |
| 142 | $4.0 \times 10^6$ | 182 | $3.0 \times 10^7$ |
| 142 | $3.5 \times 10^6$ | 191 | $4.0 \times 10^7$ |

[a] Based on a comparison of measured EPR spectra and spectra simulated on the assumption that $a^{H_\gamma}$(syn) = 0.811 G and $a^{H_\gamma}$(anti) = 0.639 G, i.e., that $a^{H_\gamma}(syn)/a^{H_\gamma}(anti) = 1.27$ (see text).

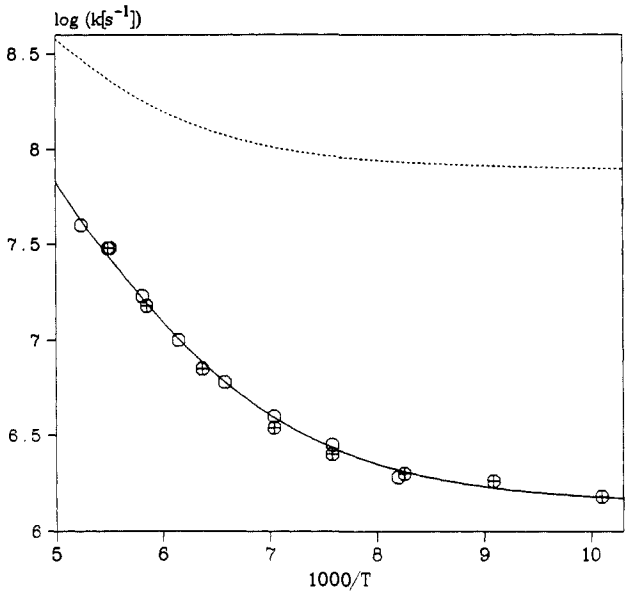


**Figure 5.** Arrhenius plot for the inversion of [2-D]-1,3-dioxolan-2-yl. Crossed and uncrossed circles refer to different sets of measurements. The probable error in the log $k$ values obtained from Table II is ca. ±0.1 log unit. The solid line depicts calculated rate constants for the potential of eq 1 with parameter values $A^D$ = 9.38 $cm^{-1}$, $B^D$ = 280 $cm^{-1}$. The broken line depicts corresponding rate constants calculated for the nondeuterated radical ($A^H$ = 14.16 $cm^{-1}$, $B^H$ = 344 $cm^{-1}$).[21]

[2-D]-1,3-dioxolan-2-yl radical are masked. However, the hfs of both radicals can be readily determined (see Table I).

The EPR spectrum of [2-D]-1,3-dioxolan-2-yl shows a strong temperature dependence (see Figure 4). At 182 K, the triplet of quintets indicates rapid inversion on the EPR time scale. As the temperature was lowered, selective line broadening became evident. Unfortunately, even at 99 K, the lowest temperature at which the spectrum was reasonably well resolved, the radical did not achieve a frozen configuration that would have permitted accurate measurement of the hfs of the two pairs of inequivalent γ-hydrogens. That is, we could measure the sum $a^{H_\gamma}$(syn) + $a^{H_\gamma}$(anti), but not the two individual hfs, which are required for spectral simulation. Fortunately, for the 2-methyl-1,3-dioxolan-2-yl radical, the $a^{H_\gamma}(syn)/a^{H_\gamma}(anti)$ ratio is known to have a value of ca. 1.4.[16] By trial and error we found that a ratio of 1.27 gives the best agreement between the observed and simulated EPR spectra (see Figure 4). The derived rate constants for inversion, $k^{D}_{inv}$, (which are based on this ratio) are given in Table II and have been plotted according to the Arrhenius equation in Figure 5. This plot is strongly curved and indicates a limiting rate constant of ca. $1.1 \times 10^6$ $s^{-1}$ at $T$ = 0 K. Taken together with the large isotope effect (which follows from the observation that $k^{H}_{inv} \gtrsim 10^8$ $s^{-1}$ over the same temperature range), this confirms that inversion proceeds by quantum-mechanical tunneling.

(16) Reference 13 gives 1.24/0.91 = 1.36, and refs 11 and 14 give 1.45/1.00 = 1.45. Assignment of the larger hfs to $H_\gamma$ (syn) is based on INDO calculations (see ref 11).

**Table III.** UHF-6-31 G** 1,3-Dioxolan-2-yl Radical Optimized Geometries[a]

| | $C_{2v}$ | $C_2$ | $C_1$ |
|---|---|---|---|
| $C_1H_2$ | 1.062 | 1.062 | 1.078 |
| $C_5H_7$ | 1.083 | 1.081 | 1.082 |
| $C_5H_9$ | 1.083 | 1.086 | 1.086 |
| $C_6H_8$ | 1.083 | 1.081 | 1.081 |
| $C_6H_{10}$ | 1.083 | 1.086 | 1.086 |
| $C_1O_3$ | 1.356 | 1.358 | 1.364 |
| $C_1O_4$ | 1.356 | 1.358 | 1.360 |
| $O_3C_5$ | 1.407 | 1.409 | 1.411 |
| $O_4C_6$ | 1.407 | 1.409 | 1.407 |
| $C_5C_6$ | 1.540 | 1.525 | 1.525 |
| $H_2C_1O_3O_4$ | 0 | 0 | 41.99 |
| $C_1O_4C_6C_5$ | 0 | 25.08 | 31.10 |
| $C_6C_5O_3C_1$ | 0 | 25.08 | 14.36 |

[a] Bond lengths in Å, angles in degrees.

**Table IV.** UHF-6-31G** Energies and Zero-Point Energies of the 1,3-Dioxolan-2-yl Radical and its 2-D Isotopomer

| configuration | energy, au | zpe,[a] $cm^{-1}$ | $\Delta E$, kcal/mol |
|---|---|---|---|
| $C_{2v}$(α-H) | −266.16329 | 18347 | 8.78 |
| (α-D) | | 17696 | 8.76 |
| $C_2$(α-H) | −266.16572 | 18500 | 7.29 |
| (α-D) | | 17842 | 7.32 |
| $C_1$(α-H) | −266.17768 | 18424 | 0 |
| (α-D) | | 17780 | 0 |

[a] "Tunneling" mode excluded.

**Quantum-Chemical Calculations.** As in our earlier work,[6,7] we use an ab initio molecular orbital method to calculate the structure and vibrational force field of the radical. Using the GAMESS program,[17] we optimized the geometry and calculated the normal-mode coordinates and frequencies at the UHF/6-31G** level of theory[18] for stationary points of the potential-energy surface relevant to the inversion process. Full geometry optimization leads to an asymmetric ($C_1$) equilibrium structure. Four equivalent equilibrium configurations involving two potential-energy barriers can be recognized by inspection: one barrier is associated with inversion and the other with ring puckering.[19] If the radical is constrained to a $C_{2v}$ conformation with a planar ring and the $C_\alpha$–$H_\alpha$ (or $C_\alpha$–$D_\alpha$) bond in the plane of the ring, the stationary point, i.e., the zero-gradient conformation on the potential-energy surface, turns out to be a saddle point of order three. That is, the energy Hessian, calculated with respect to the nuclear displacements, is characterized by three negative eigenvalues, which correspond to three imaginary frequencies. One of these involves the inversion and the other two, which are of much lower frequency, concern out-of-plane ring vibrations. If the symmetry is allowed to relax to $C_2$ with the $C_\alpha$–$H_\alpha$ (or $C_\alpha$–$D_\alpha$) bond along the 2-fold axis, only one imaginary frequency remains, namely, that of the inversion. Hence this $C_2$ configuration corresponds to the transition state of the inversion process.

The optimized geometries of the three configurations mentioned above are listed in Table III. The energies and zero-point energies of 1,3-dioxolan-2-yl and its 2-D isotopomer are listed in Table IV. We note that the calculated inversion barrier is close to the observed barrier of 5.65 kcal/mol in 2-methyl-1,3-dioxolan-2-yl.[13,14] The vibrational frequencies, $\omega_k$, of the two isotopomers in the $C_1$ equilibrium configuration are given in Table V. Although no experimental frequencies are available, the values of, for example, the CH-stretch frequencies suggest that the usual scaling factor of ~0.9 applies to the calculated frequencies.[20] The

(17) Dupuis, M.; Spangler, D.; Wendoloski, J. J. NRCC Software Catalogue Program QG01, 1980. Revised by Schmidt, M. W.; Baldridge, K. K.; Boatz, J. A.; Koseki, S.; Gordon, M. S.; Elbert, S. T.; Lam, B. T. *QCPE* **1987**, *No. 7*, 115.
(18) Francl, M. M.; Pietro, W. J.; Hehre, W. J.; Binkley, J. S.; Gordon, M. S.; De Frees, D. J.; Pople, J. A. *Chem. Phys.* **1982**, *77*, 3654–3665. Hariharan, P. C.; Pople, J. A. *Theor. Chim. Acta* **1973**, *28*, 213–222.
(19) Cremer, D.; Pople, J. A. *J. Am. Chem. Soc.* **1975**, *97*, 1354–1358.
(20) Hehre, W. J.; Radom, L.; Schleyer, P. v. R.; Pople, J. A. *Ab Initio Molecular Orbital Theory*; Wiley: New York, 1986.

**Table V.** Calculated (Prior to Scaling by Factor 0.89)[20] Normal-Mode Frequencies ($cm^{-1}$) of 1,3-Dioxolan-2-yl and its 2-D Isotopomer for the $C_1$ Equilibrium Conformation

| $(\alpha\text{-H})\omega_k$ | assignment | $(\alpha\text{-D})\omega_k$ |
|---|---|---|
| 163 | CH(D) pyr, $OCH_{(2)}$[a] | 163 |
| 266 | CH(D) pyr, $OCH_{(2)}$[a] | 266 |
| 725 | $OCH_{(2)}$ | 725 |
| 828 | COC//COC, COD pyr | 818 |
| 962 | $OCH_{(2)}$ | 995 |
| 1028 | CC | 1028 |
| 1081 | OCH(D) pyr[b] | 880 |
| 1087 | $C_{5,6}O$ | 1093 |
| 1118 | $C_1H$ pyr//$OC_{5,6}$ | 1184 |
| 1249 | $OC_{3,4}$, OCH//OCH | 1256 |
| 1272 | $OCH_{(2)}$ | 1282 |
| 1331 | $OC_1$ | 1315 |
| 1336 | $OCH_{(2)}$ | 1348 |
| 1369 | $OCH_{(2)}$ | 1372 |
| 1415 | CH(D) wag | 906 |
| 1527 | OCH | 1525 |
| 1541 | OCH | 1529 |
| 1654 | OCH | 1654 |
| 1669 | OCH | 1669 |
| 3193 | CH stretch | 3193 |
| 3223 | CH stretch | 3222 |
| 3273 | CH stretch | 3272 |
| 3292 | CH stretch | 3292 |
| 3326 | CH(D) stretch | 2454 |

[a] $C_\alpha$ "out of plane" bending modes facilitating hydrogen tunneling. [b] "Tunneling" mode.

**Table VI.** Calculated (Unscaled) Normal-Mode Frequencies ($cm^{-1}$) and Displacement Parameters [Å $(amu)^{1/2}$] of 1,3-Dioxolan-2-yl and its 2-D Isotopomer for the $C_2$ Symmetry Conformation

| | α-H | | | α-D | |
|---|---|---|---|---|---|
| sym | $\Delta_k$ | $\omega_k$ | assignment | $\omega_k$ | $\Delta_k$ |
| a | 0.155 | 244 | ring, $OCH_{(2)}$[a] | 244 | 0.149 |
| | 0.075 | 828 | OCO | 821 | 0.057 |
| | | 1021 | CC, $OCH_{(2)}$ | 1021 | |
| | 0.027 | 1096 | COC | 1080 | 0.060 |
| | 0.016 | 1258 | $OCH_{(2)}$ | 1258 | 0.025 |
| | 0.019 | 1322 | CO | 1298 | 0.043 |
| | 0.016 | 1368 | HCH | 1368 | 0.017 |
| | | 1524 | $CH_2$ wag | 1524 | |
| | | 1664 | $CH_2$ scissors | 1664 | |
| | | 3221 | CH stretch | 3221 | |
| | | 3284 | CH stretch | 3284 | |
| | 0.123 | 3490 | CH(D) stretch | 2592 | 0.164 |
| b | 0.620 | 1048i | CH(D) pyr[b] | 862i | 0.754 |
| | 0.173 | 168 | CH(D) pyr, ring[a] | 152 | |
| | | 714 | CC, $OCH_{(2)}$ | 711 | |
| | 0.009 | 964 | OCH, $OCH_{(2)}$, OCD | 881 | 0.008 |
| | 0.017 | 1095 | $OCH_{(2)}$, OCH(D) | 1001 | 0.010 |
| | | 1283 | OCH(D) | 1180 | |
| | | 1327 | OCH(D), $OCH_{(2)}$ | 1314 | |
| | | 1406 | $OCH_{(2)}$, OCH(D) | 1366 | |
| | | 1552 | OCH, $CH_2$ wag//$CH_2$ wag | 1535 | |
| | | 1652 | $CH_2$ scissors | 1652 | |
| | | 3221 | CH stretch | 3221 | |
| | | 3296 | CH stretch | 3296 | |

[a] $C_\alpha$ "out of plane" bending modes facilitating hydrogen tunneling. [b] "Tunneling" mode.

scaled frequencies of the $H_\alpha$ and $D_\alpha$ tunneling modes are then calculated to be 973 and 792-$cm^{-1}$, respectively.

The vibrational frequencies $\omega_k$ (unscaled) and the corresponding vibrational displacement parameters, $\Delta_k$, for the $C_2$ and $C_{2v}$ conformations are given in Tables VI and VII, respectively. Here $\Delta_k$ is given by

$$\Delta_k = \sum_i m_i^{1/2} r_i \mathbf{L}_{ik}$$

where $m_i^{1/2} r_i$ are mass-weighted atomic displacements and $\mathbf{L}$ is

(21) Note that $A^D = (\omega^D/\omega^H)^2 A^H$; the exponent 2 is missing from the corresponding formula in ref 6 (p 6725).

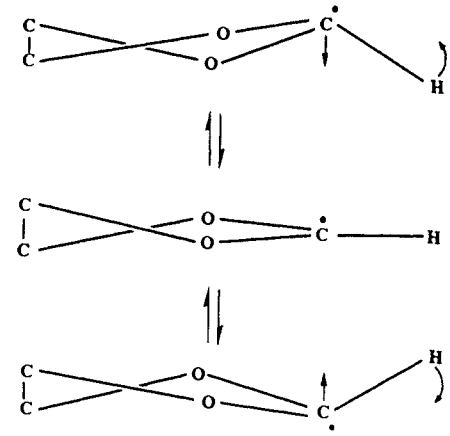

**Figure 6.** Mechanism of inversion of 1,3-dioxolan-2-yl. The three portions in this side-on view refer to the initial, transition, and final states, respectively. For clarity the vertical amplitudes have been enlarged and the transition-state configuration has been rotated slightly with respect to the equilibrium configurations.

the $3N \times (3N - 6)$ matrix that relates the normal coordinates to the mass-weighted atomic Cartesian coordinates. The $H_\alpha$ and $D_\alpha$ tunneling modes dominate the displacement between the $C_2$ and $C_1$ structures but, as expected, there are also nonnegligible contributions from low-frequency ring-bending modes and from the $C_\alpha$–$H_\alpha$ or $C_\alpha$–$D_\alpha$ stretching mode.

**Inversion Rate Constants.** The inversion process is illustrated via a side-on view of the radical in Figure 6. The $C_\alpha$ and $H_\alpha$ atoms move in opposite directions in the plane of the paper while the remaining atoms move very little. In the transition state, the $C_\alpha$ and $H_\alpha$ atoms and the molecular center of mass lie on a straight line. The inversion is therefore "double-hinged" so that the $C_\alpha$ motion reduces the $H_\alpha$ (or $D_\alpha$) tunneling path length compared, for example, to the oxiranyl radical,[6] leading to faster tunneling although the barrier heights for these two radicals (vide infra) are not very different. This, combined with the shorter path, implies that the curvature at the top of the barrier is greater for the dioxolanyl than for the oxiranyl radical, as is reflected in the higher $C_\alpha$–$H_\alpha$ imaginary frequency for the former radical (viz 1048i vs 999i $cm^{-1}$ for oxiranyl[6]).

For the oxiran-2-yl radical, the tunneling rate and its temperature and isotope dependence could be reasonably well described by a potential of the form[6]

$$V(q) = (Aq^4 - Bq^2)[1 - \exp(-q^2)] \quad (1)$$

where $q$ is the (dimensionless) $H_\alpha$ inversion coordinate and $A$ and $B$ are close to their values calculated by quantum-chemical methods. For the 1,3-dioxolan-2-yl radical the tunneling path and hence the inversion coordinate depends on the $C_\alpha$ coordinate, so that a one-dimensional tunneling calculation may be expected to be less successful. This is indeed the case. Thus, although a very good fit to the kinetic data of Table II can be obtained with eq 1 (as shown in Figure 5), a comparison of the empirical and calculated parameters (see Table VIII) and of the resulting potential-energy function (Figure 7) indicates discrepancies much larger than for the oxiranyl radical. For example, the empirical inversion frequency of 560 $cm^{-1}$ is much lower than its calculated value of 790 $cm^{-1}$ and similar to the empirical value of 549 $cm^{-1}$ for [2-D]oxiranyl,[6] contrary to the quantum-chemical predictions.

These discrepancies indicate the need for an improved model in which low-frequency $C_\alpha$-bending modes are included. Since the harmonic frequency of these modes is calculated to be nearly the same in the $C_1$ and $C_2$ conformations, there is no evidence of harmonic mixing with the inversion mode between these conformations. The interaction must therefore be anharmonic. For simplicity we limit ourselves to a single $C_\alpha$ out of plane bending mode and label its (dimensionless) coordinate by $Q$. The lowest order anharmonic coupling term will then be of the form $q^2Q^2$, since the $qQ^2$ and $q^2Q$ terms are forbidden under $C_2$ symmetry. If we take the effective $C_\alpha$ mode to be harmonic with a frequency

**Table VII.** Calculated (Unscaled) Normal-Mode Frequencies ($cm^{-1}$) and Displacement Parameters [Å $(amu)^{1/2}$] of 1,3-Dioxolan-2-yl Radical and its 2-D Isotopomer for the $C_{2v}$ Symmetry Conformation

| | α-H | | | | α-D | | |
|---|---|---|---|---|---|---|---|
| sym | $\Delta_k(C_2)$ | $\Delta_k(C_1)$ | $\omega_k$ | assignment | $\omega_k$ | $\Delta_k(C_1)$ | $\Delta_k(C_2)$ |
| $a_1$ | 0.053 | 0.118 | 835 | OCO, COC | 829 | 0.095 | 0.047 |
| | 0.213 | 0.166 | 1028 | $CH_2$ wag, CC | 1025 | 0.186 | 0.217 |
| | 0.044 | 0.072 | 1102 | OCO, $C_1O$ | 1088 | 0.079 | 0.023 |
| | 0.029 | | 1338 | $C_1O$ | 1315 | 0.020 | 0.037 |
| | 0.045 | 0.030 | 1522 | $CH_2$ wag | 1521 | 0.028 | 0.045 |
| | | 0.005 | 1678 | $CH_2$ scissors | 1678 | | 0.008 |
| | 0.135 | 0.107 | 3239 | CH | 3239 | 0.110 | 0.135 |
| | | 0.124 | 3492 | $C_1H(D)$ | 2594 | 0.161 | |
| $a_2$ | 1.461 | 1.313 | 197i | ring, $CH_2$[a] | 197i | 1.313 | 1.461 |
| | | | 1256 | $OCH_{(2)}$ | 1256 | | |
| | 0.014 | 0.012 | 1358 | $CH_2$ bend | 1358 | 0.012 | 0.014 |
| | | | 3262 | CH stretch | 3262 | | |
| $b_1$ | | 0.620 | 1073i | OOCH pyr[b] | 889i | 0.749 | |
| | | 0.165 | 111i | ring, OOCH pyr[a] | 102i | | |
| | | | 912 | $CH_2$ bend, ring | 912 | | |
| | | 0.013 | 1340 | $CH_2$ bend | 1340 | 0.013 | |
| | | | 3288 | CH stretch | 3288 | | |
| $b_2$ | | | 796 | CC, CH(D) wag | 782 | | |
| | | 0.049 | 1084 | CH(D) wag | 917 | | |
| | | 0.011 | 1310 | OCH(D) | 1196 | 0.069 | |
| | | 0.054 | 1399 | OCH(D), $CH_2$ wag | 1354 | 0.044 | |
| | | 0.031 | 1567 | $CH_2$ wag | 1551 | 0.022 | |
| | | | 1660 | $CH_2$ scissors | 1660 | | |
| | | 0.019 | 3227 | CH stretch | 3227 | 0.019 | |

[a] $C_\alpha$ "out of plane" bending modes facilitating hydrogen tunneling. [b] "Tunneling" mode.

**Table VIII.** Comparison of the Characteristics of the ab Initio and Empirical Potentials for the Inversion of [2-*D*]-1,3-Dioxolan-2-yl and (in parentheses) 1,3-Dioxolan-2-yl

| | ω(bottom),[a] $cm^{-1}$ | ω(top),[a] $cm^{-1}$ | pyramid angle, deg | barrier ht, $cm^{-1}$ |
|---|---|---|---|---|
| scaled ab initio | 790 (973) | 775 (943) | 42.0 | 2544 |
| empirical, eq 1 | 560 (688) | 560 (688) | 42.2 | 2090 |
| empirical, eq 3 | 685 (842) | 685 (842) | 43.7 | 2680 |

[a] Obtained from the second derivative of the potential at the stationary point.

$\Omega = 140\ cm^{-1}$ corresponding to a potential $^1/_2\Omega Q^2$ (in frequency units), the two-dimensional potential governing inversion will be of the form

$$V(q,Q) = (Aq^4 - Bq^2)[1 + \exp(-q^2)] + \tfrac{1}{2}\Omega Q^2 + Fq^2Q^2 \quad (2)$$

Although the corresponding Schrödinger equation can be readily solved by numerical means, optimization of the parameters $A$, $B$, and $F$ will be laborious. Moreover, it is not immediately clear how to arrange the resulting eigenvalues into pairs of levels split by tunneling. In the absence of experimental data on the magnitude of the deuterium effect, a short-cut therefore appears warranted. To this end we rewrite eq 2 in the pseudo-one-dimensional form

$$V_n(q;Q) = [Aq^4 - (B + FQ_n^2)q^2][1 + \exp(-q^2)] \quad (3)$$

where $Q_n$ is the classical turning point of the $C_\alpha$ oscillator in its $n$th state:

$$Q_n^2 = 2E_n(Q)/\Omega = 2n + 1 \quad (4)$$

Thus we have a series $V_0$, $V_1$, $V_2$, ... of inversion potentials whose contributions to the inversion we weight according to their Boltzmann factors $\exp(-n\hbar\Omega/k_BT)$.

The results can be fitted perfectly to the available data, as shown in Figure 8. Contrary to the equally good fit of Figure 5, this does not require major adjustment of the calculated parameters, as can be seen from Table VIII. In particular, the inversion frequency is now higher than that for [2-D]oxiranyl as predicted quantum-chemically. In Figure 9, the calculated potential is compared with the empirical potential evaluated for $F = 0$, corresponding to the stationary points at which the quantum-chemical calculations were carried out.

The effect of the anharmonic cross-term on the inversion rate can be deduced from a comparison of the curve that fits the data

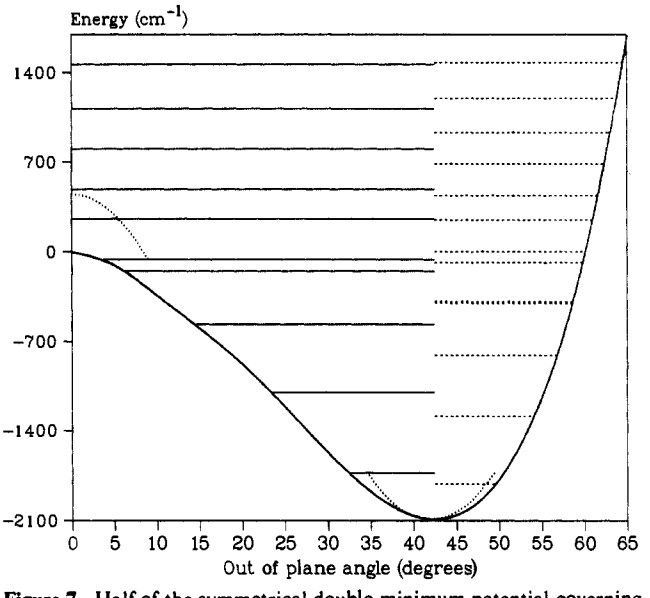


**Figure 7.** Half of the symmetrical double-minimum potential governing the inversion of 1,3-dioxolan-2-yl plotted against the out of plane angle. The solid curve depicts the empirical potential obtained by fitting the observed rate constants by means of the potential of eq 1, as in Figure 5. The broken curves depict calculated parts of the potential. Horizontal solid and broken lines depict the energy levels associated with the solid-curve potential for 1,3-dioxolan-2-yl and [2-D]-1,3-dioxolan-2-yl, respectively.

points with the lower broken curve, calculated for $F = 0$. The cross-term, which is negative, leads to a decrease of both the tunneling distance

$$\Delta q \simeq 2q \simeq 2[B/A + (2n + 1)F/A]^{1/2} \quad (5)$$

and the barrier height

$$E_b \simeq [B + (2n + 1)F]^2/2A \quad (6)$$

with increasing $n$, i.e., with increasing temperature.

Figures 5 and 8 also show how the inversion rate constant calculated for the nondeuterated radical depends on temperature. Although no experimental rate constants are available for the nondeuterated radical, the calculated values are high enough to

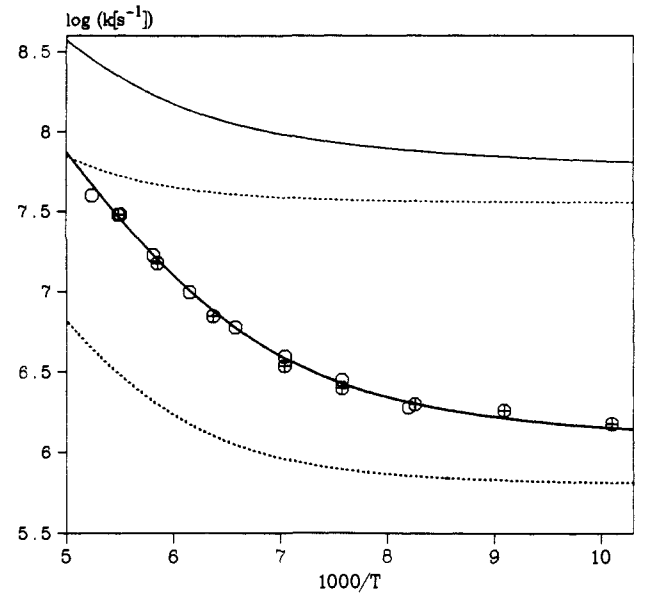


**Figure 8.** As with Figure 5, except that the curves have been calculated from the potential of eq 3 with (for [2-D]dioxolan-2-yl) $A^D = 10.95$ cm$^{-1}$, $B^D = 342$ cm$^{-1}$, $F^D = -8.55$ cm$^{-1}$ (solid lower curve), and $F^D = 0$ (broken lower curve). The upper curves are for the nondeuterated radical ($A^H = 16.53$ cm$^{-1}$, $B^H = 421$ cm$^{-1}$, $F^H = -10.53$ and 0 cm$^{-1}$).[21]

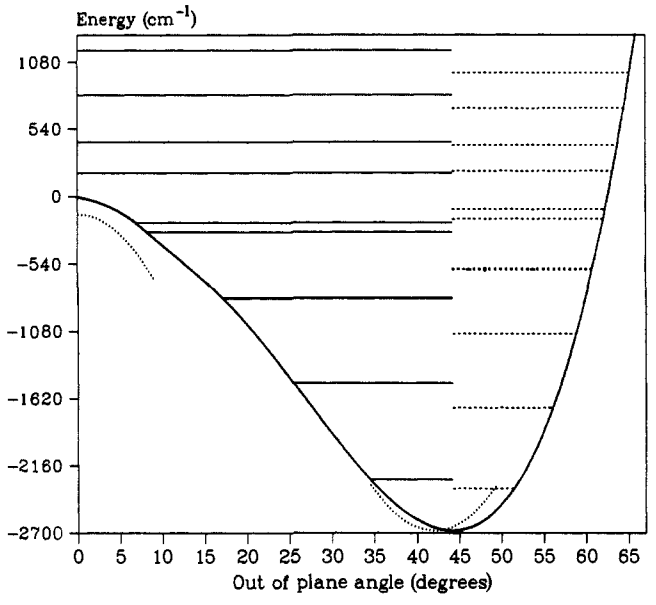


**Figure 9.** As with Figure 7 for the potential of eq 3 with $F = 0$ (broken curve).

explain the absence of line broadening in the EPR experiments. Both Figures 5 and 8 predict essentially the same inversion rate constants for 1,3-dioxolan-2-yl. In the case of the oxiran-2-yl and [2-D]oxiran-2-yl radicals, we found such predictions to be accurate and so we expect them to be close in the present case as well.

## Discussion

The 1,3-dioxolan-2-yl radical has two equivalent nonplanar equilibrium configurations between which it oscillates rapidly. In solution this oscillation will be damped by solvent interactions and can be described effectively as a dynamic equilibrium between the two configurations. This picture allows an accurate reproduction of the observed temperature dependence of the EPR signal. Similar observations apply to the radicals cyclopropyl,[4] 1-methylcyclopropyl,[5,7] and oxiran-2-yl,[6] which we studied previously. In all these radicals, the potential along the inversion coordinate exhibits a symmetrical double minimum. This makes it possible to relate the inversion rate to the level splitting. Strictly speaking, this splitting relates to the inversion frequency rather than the

**Table IX.** Structural and Kinetic Parameters on Inversion of Some Cyclic Radicals

| radical | pyramid angle deg | barrier ht (calcd) $\Delta E$, kcal/mol | $k_{inv}(T = 353$ K), s$^{-1}$ | $k_{inv}(T = 0$ K), s$^{-1}$ |
|---|---|---|---|---|
|  | 39.3[a] | (3.0)[a] | $8.2 \times 10^{11}$[b] | $1.4 \times 10^{11}$[b] |
|  | | | $5.1 \times 10^{11}$[b] | $1.8 \times 10^{10}$[b] |
|  | 39.5[c] | 3.1,[d] 3.6[e] (4.3)[c] | $1.0 \times 10^{11}$[e] | $3.3 \times 10^{4}$[c,e] |
|  | 45.1[f,g] | 6.8[f] (9.0)[f] | $4.4 \times 10^{9}$[f] | $6.7 \times 10^{6}$[f] |
|  | | (8.9)[f] | $2.6 \times 10^{9}$[f] | $6.9 \times 10^{4}$[f] |
| 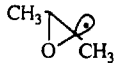 | | 5.6,[h] 7.0[f,i] | $1.0 \times 10^{9}$[h] | |
|  | 42.0 | 7.7 (7.3) | $1.6 \times 10^{10}$ | $5.4 \times 10^{7}$ |
|  | | (7.3) | $9.9 \times 10^{9}$ | $1.1 \times 10^{6}$ |
|  | | 5.6,[j] 5.7[k] | $5.4 \times 10^{9}$[j] | |

[a] Dupuis, M.; Pacansky, J. *J. Chem. Phys.* **1982**, *76*, 2511–2515. [b] Calculated by using the empirical frequency $C_\alpha$–$H_\alpha$ or $C_\alpha$–$D_\alpha$ of the oxiran-2-yl counterpart[6] and a barrier height of 3.0 kcal/mol. [c] Calculated according to or taken from ref 7. [d] Reference 5. [e] Upper limit; obstruction from hindered rotation of methyl group is neglected. [f] Calculated according to or taken from ref 6. [g] Corrected value; the value of 56.5 given in ref 6 is in error, see: Zerbetto, F.; Zgierski, M. Z. *Chem. Phys.*, **1989**, *139*, 503–506. [h] Itzel, H.; Fischer, H. *Helv. Chim. Acta* **1976**, *59*, 880–901. [i] Corrected for zero-point energy. [j] Reference 13. [k] Reference 14.

inversion rate. Similarly, the EPR line shape can be explained in terms of a periodic process instead of a dynamic equilibrium. It seems therefore that the conventional description in terms of rate processes may be avoidable. We shall assume, however, that this description is justified because of the interaction with the solvent.

The relation between the inversion rate and the level splitting is simple only for a one-dimensional inversion potential, as in the case of the oxiran-2-yl radical. For the other two radicals investigated, the inversion potential turned out to be essentially two-dimensional. In the case of the 1-methylcyclopropyl radical, the inversion is strongly coupled to methyl rotation. However, an effectively one-dimensional inversion potential could be obtained in the temperature range where experimental data are available. It is based on the observation that, except for the lower limit of this range, the methyl rotation is so fast that its effect is averaged out.

In the case of 1,3-dioxolan-2-yl, the inversion mode is strongly coupled to an "out-of-plane" ring-bending mode. To achieve reduction to an effectively one-dimensional potential, we assumed that the kinetic energy of this low-frequency mode can be neglected and that the inversion will occur when this mode is in its classical turning point, namely, the one that minimizes the hydrogen tunneling distance. This approach turns out to be satisfactory for the limited set of data available. In principle, it is not difficult, however, to generalize our approach to 2 degrees of freedom. In particular, if the two vibrations are only weakly coupled, as they are for dioxolanyl, numerical solution is straightforward. The two-dimensional Schrödinger equation can be readily solved in terms of a suitable basis set. If this is done for a range of values of the coupling parameter $F$, it will be easy to recognize the split level pairs. The coupling parameter giving the best fit to the observed rate constants can then be determined by interpolation. The coupling obtained in this way may differ somewhat from the

coupling obtained in our quasi-one-dimensional approach, but since no experimental value is available, we have not pursued this point. Of course the calculation would be much more difficult for a coupling strong enough to change the level splittings by amounts comparable to the level spacings.

Table IX summarizes the results obtained thus far by ourselves and others on the inversion of free radicals in which the radical center is part of a small ring with or without heteroatoms. The rate constants listed for 353 and 0 K are calculated ("extrapolated") from the available experimental data by means of a quasi-one-dimensional procedure based on the calculation of level splittings. This method is found to be reliable for the systems studied. We therefore conclude that the method of vibronic level splittings, when properly adjusted for contributions of additional degrees of freedom, is satisfactory for tunneling rates in the range measurable by EPR techniques.

# Efficiencies of Photoinduced Electron-Transfer Reactions: Role of the Marcus Inverted Region in Return Electron Transfer within Geminate Radical-Ion Pairs

**Ian R. Gould,* Deniz Ege, Jacques E. Moser,† and Samir Farid***

*Contribution from the Eastman Kodak Company, Corporate Research Laboratories, Rochester, New York 14650-2109.* *Received November 24, 1989*

**Abstract:** In photoinduced electron-transfer processes the primary step is conversion of the electronic energy of an excited state into chemical energy retained in the form of a redox (geminate radical-ion) pair ($A + D \xrightarrow{h\nu} A^{\bullet-}/D^{\bullet+}$). In polar solvents, separation of the geminate pair occurs with formation of free radical ions in solution. The quantum yields of product formation, from reactions of either the free ions, or of the geminate pair, are often low, however, due to the return electron transfer reaction ($A^{\bullet-}/D^{\bullet+} \rightarrow A + D$), an energy-wasting step that competes with the useful reactions of the ion pair. The present study was undertaken to investigate the parameters controlling the rates of these return electron transfer reactions. Quantum yields of free radical ion formation were measured for ion pairs formed upon electron-transfer quenching of the first excited singlet states of cyanoanthracenes by simple aromatic hydrocarbon donors in aceonitrile at room temperature. The free-ion yields are determined by the competition between the rates of separation and return electron transfer. By assuming a constant rate of separation, the rates of the return electron transfer process are obtained. These highly exothermic return electron transfer reactions ($-\Delta G_{-et}$ = 2–3 eV) were found to be strongly dependent on the reaction exothermicity. The electron-transfer rates showed a marked *decrease* (ca. 2 orders of magnitude in this $\Delta G_{-et}$ range) with *increasing* exothermicity. This effect represents a clear example of the Marcus "inverted region". Semiquantum mechanical electron-transfer theories were used to analyze the data quantitatively. The electron-transfer rates were found also to depend upon the degree of charge delocalization within the ions of the pair, which is attributed to variations in the solvent reorganization energy and electronic coupling matrix element. Accordingly, mostly on the basis of redox potentials, one can vary the quantum yield of free-ion formation from a few percent to values approaching unity. Use of a strong donor with a strong acceptor to induce reactions based on electron transfer is likely to be inefficient because of the fast return electron transfer in the resulting low-energy ion pair. A system with the smallest possible driving force for the initial charge-separation reaction results in a high-energy, and therefore long-lived ion pair, which allows the desired processes to occur more efficiently. The use of an indirect path based on secondary electron transfer, a concept called "cosensitization", results in efficient radical-ion formation even when the direct path results in a very low quantum yield.

## I. Introduction

Many examples of photoinduced electron-transfer reactions of organic molecules have been identified.[1] For efficient reaction, the excited-state energy of the species that absorbs the light, either the donor or the acceptor, should be higher than the energy required to reduce the acceptor to its radical anion and oxidize the donor to its radical cation. This situation is illustrated in Scheme I for the case of a singlet excited acceptor A in the presence of a donor D. For such reactions it is well-known that second-order electron-transfer quenching of the excited state by the redox partner occurs efficiently to form primary charge-separated species such as exciplexes and solvated geminate radical-ion pairs ($k_{et}$, Scheme I).[2] Very often these reactions are performed in polar solvents (usually acetonitrile) to facilitate the solvation of the primary geminate radical-ion pairs into free radical ions in solution ($k_{sep}$, Scheme I). The chemical products of reactions under these conditions are typical of those expected for free radical ions.[1] The maximum quantum yield for such reactions, in the absence of chain amplification or chemical reaction within the geminate radical-ion pairs, is thus given by the quantum yield

Scheme I. Energy Diagram for Photoinduced Electron Transfer

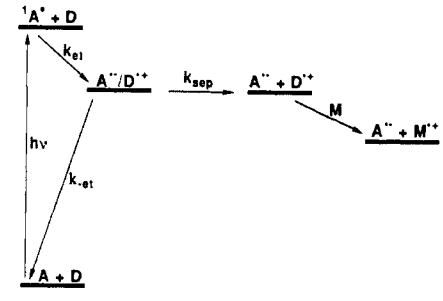


for formation of the free radical ions via solvation and separation processes.[1a,3] However, solvation and separation of the radical

†Current address: Institut de Chimie Physique, Ecole Polytechnique Fédérale, CH-1015 Lausanne, Switzerland.

(1) (a) Mattes, S. L.; Farid, S. In *Organic Photochemistry*; Padwa, A., Ed.; Marcel Dekker: New York, 1983; Vol. 6, p 233. (b) Davidson, R. S. In *Advances in Physical Organic Chemistry*; Gold, V., Bethell, D., Eds.; Academic Press: London, 1983; Vol. 19, p 130. (c) Mattes, S. L.; Farid, S. *Science* **1984**, *226*, 917. (d) Kavarnos, G. J.; Turro, N. J. *Chem. Rev.* **1986**, *86*, 401. (e) *Photoinduced Electron Transfer, Part C. Photoinduced Electron Transfer Reactions: Organic Substrates*; Fox, M. A., Chanon, M., Eds.; Elsevier: Amsterdam, 1988. (f) Mattay, J. *Synthesis* **1989**, 233.

0002-7863/90/1512-4290$02.50/0 